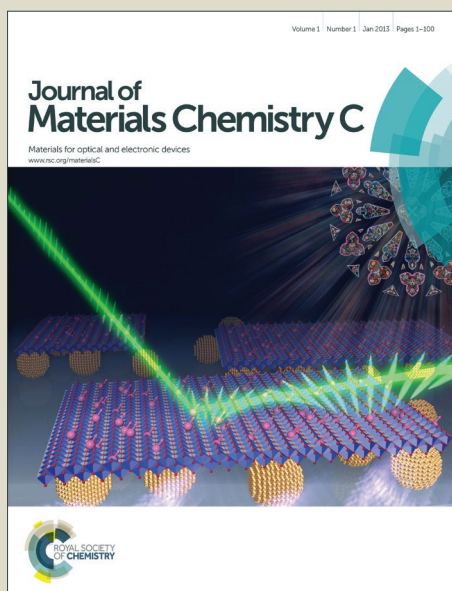


Journal of Materials Chemistry C

Accepted Manuscript



This article can be cited before page numbers have been issued, to do this please use: J. Lu, Q. Zhang, H. Zhuang, J. H. He, S. Xia, H. Li, N. Li and Q. Xu, *J. Mater. Chem. C*, 2015, DOI: 10.1039/C5TC00839E.



This is an *Accepted Manuscript*, which has been through the Royal Society of Chemistry peer review process and has been accepted for publication.

Accepted Manuscripts are published online shortly after acceptance, before technical editing, formatting and proof reading. Using this free service, authors can make their results available to the community, in citable form, before we publish the edited article. We will replace this *Accepted Manuscript* with the edited and formatted *Advance Article* as soon as it is available.

You can find more information about *Accepted Manuscripts* in the [Information for Authors](#).

Please note that technical editing may introduce minor changes to the text and/or graphics, which may alter content. The journal's standard [Terms & Conditions](#) and the [Ethical guidelines](#) still apply. In no event shall the Royal Society of Chemistry be held responsible for any errors or omissions in this *Accepted Manuscript* or any consequences arising from the use of any information it contains.



Journal Name

ARTICLE

Improved ternary memory performance of donor-acceptor structured molecules through cyano substitution

Qijian Zhang, Hao Zhuang, Jinghui He, Shugang Xia, Hua Li,* Najun Li, Qingfeng Xu and Jianmei Lu*

Received 00th January 20xx,
Accepted 00th January 20xx

DOI: 10.1039/x0xx00000x

www.rsc.org/

Organic memory devices can greatly increase the data-storage density and have attracted more and more attentions. Thus, two small molecules DPHCANA and DPCNCANA were designed and successfully synthesized to investigate the improvement of the memory device through introducing the strong electron withdrawing group cyano on the central phenyl ring. It is noteworthy that DPCNCANA with cyano exhibited excellent ternary memory behavior benefited from induced intermolecular H-bond connection and layer by layer molecular stacking in film state, which counteracted the higher hole transport barrier lying between the film and the bottom electrode. In addition, we have also found that the additional cyano group substitution lower the LUMO energy level, which is favorable to the stability in the air ambient circumstance. We envisage that this study present here is very useful to the rational design of advanced next-generation semiconductor materials.

Introduction

Over the past decade, small molecular and polymeric materials have attracted more and more attentions as alternatives to traditional inorganic optical or magnetic materials in binary data storage applications due to several attractive merits as low cost, well-defined structure, easy processing, 3D stacking and super-high data-storage density.¹⁻⁶ Our group has reported a series of ternary data storage materials and devices, which are sure to dramatically improve the data storage density when compared with the traditional binary system.⁷⁻¹⁰ During this process we proposed the “charge trap” mechanism as principle for designing multi-levels data storage materials, in which we believe that two different electron acceptors distributed in the conjugated molecular backbone served as shallow and deep charge traps is the pre-condition to achieve ternary memory devices.⁷⁻¹⁰ As we know, the more and stronger the electron acceptors are in the molecule backbone, the lower the HOMO energy level of the molecule would be. Therefore, ternary data storage materials usually exhibit very low HOMO levels which attributed to their contained no less than two electron withdrawing groups. The decreased HOMO energy level will enlarge the energy barrier between the bottom electrode and the active film for the as-fabricated sandwiched Al/organic film/ITO devices, because most of now synthesized semiconductor materials are p-type and the

bottom ITO electrode has the fixed work function at - 4.8 eV which generally serves as anode to inject holes under electric field. Therefore, the enlarged energy barrier will definitely increase the switch voltage of the ternary device, which would not only improve the power consumption but also probably give rise to the risk of puncturing the device. Therefore, design and synthesis of ternary data storage materials without increasing threshold voltage becomes very important.

In our previous studies, we have found that well enhanced intermolecular π - π stacking,¹¹ optimization of film morphology,¹² and decreasing of the molecular energy band-gaps (E_g),¹³ are beneficial to reduce the threshold voltage of the device, the former two effects are generally decided by the molecular geometric construction and the latter is usually decided by the selected electron acceptors. Taking into account of combination above three effects into one molecule is a good solution to achieve ideal ternary data storage materials. However, the incorporation of relatively large electron acceptor groups in the conjugated backbone would distort intermolecular close packing.¹⁴ To avoid this problem, it is necessary to find one suitable electron acceptor, which would not increase the E_g much and in contrary could improve the intermolecular ordered arrangement.

Herein, we combined electron-donor Carbazole (CA) and electron acceptor Naphthalimide (NA) to form a D-A structured organic small molecule, which is an efficient way to narrow the E_g by utilizing intramolecular charge transfer (ICT) transition between the D-A units in molecular backbone. Furthermore, we combined cyano groups on the CA group to form another D-A unit, in addition, the cyano group can act as the deep charge trap while the NA group would serve as the

College of Chemistry, Chemical Engineering and Materials Science, Collaborative Innovation Center of Suzhou Nano Science and Technology, Soochow University, Suzhou 215123, China. E-mail: ljim@suda.edu.cn
Fax: +86 512 65880367; Tel: +86 512 65880368

† Electronic Supplementary Information (ESI) available: [detailed experimental procedures of the intermediates, NMR spectra of the terminal compounds and IR absorbance spectra of the both molecules.]. See DOI: 10.1039/x0xx00000x

shallow charge trap thus to satisfy the pre-condition of the ternary data storage materials. The most importance of choosing cyano group here is especially reducing HOMO without enhancing molecular band-gap, and promoting the ordered molecules arrangement in the film by CN...CN and CN...H interactions to facilitate the intermolecular charge transport.¹⁵⁻¹⁷

Experimental

Materials

Iodobenzene, 4-Fluorophenylacetonitrile, 4-Bromo-1,8-naphthalic anhydride, bis(pinacolato)diboron and Octylamine were purchased from Energy Chemical, Tetrakis(triphenylphosphine)palladium(0) was purchased from Aldrich, Carbazole, NBS (N-bromosuccinimide), Ferric Chloride, Potassium Carbonate, Potassium Acetate and all the solvents were purchased from Shanghai Chemical Reagent Co. Ltd. All chemicals were used as received without further purification. The two original compounds 9-phenyl-carbazole (1a), 4-(9H-carbazol-9-yl)benzonitrile (1b), 4-(4,4,5,5-tetramethyl-1,3,2-dioxaborolan-2-yl)-N-octyl-1,8-naphthalimide (NA) were prepared according to previously reported procedures.¹⁸⁻²⁰

Instrumentation and characterizations

¹H NMR spectra were measured on an Inova 400 MHz FT-NMR workstation. All the electrical characteristics of the devices were executed by using a HP 4145B semiconductor parameter analyzer with a HP 8110A pulse generator. Thermogravimetric analysis (TGA) were conducted on a TA Instruments Dynamic TGA 2950 at a heating rate of 10 °C min⁻¹ and under an N₂ flow rate of 50 mL min⁻¹. UV-Vis absorption spectrum was obtained with the use of a Shimadzu UV-3600 spectrophotometer. Cyclic voltammetry was performed on a CorrTest CS Electrochemical Workstation analyzer at room temperature. SEM images were measured on a Hitachi S-4700 scanning electron microscope. X-ray diffraction (XRD) pattern was taken on an X'Pert-Pro MPD X-ray diffractometer. Atomic force microscopy (AFM) measurement was carried out by using a MFP-3DTM AFM instrument in tapping mode. All electrical measurements of the device were taken at ambient conditions without any encapsulation. Calculations on the two molecules investigated in this work were carried out with the Gaussian 03 program package.²¹ Electronic properties of DPHCANA and DPCNCANA in ground state, including the electrostatic potential (ESP) surfaces and molecular energy orbitals, were calculated from the density functional theory (DFT): the Becke's three-parameter functional combined with the Lee, Yang, and Parr's correlation functional (B3LYP),²² along with the 3-21G basis set.

Synthetic procedures

General procedure for synthesis of compound 4

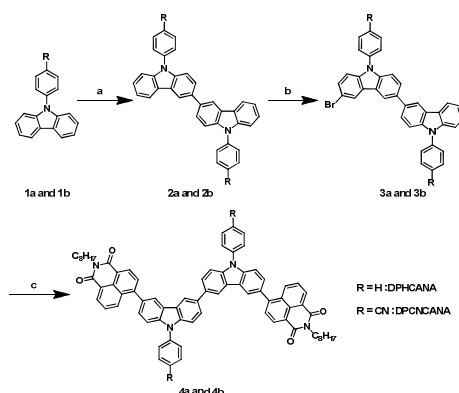
Compound 3 (0.5 mmol), 2 M potassium carbonate aqueous solution and compound 6 (0.47 g, 1.1 mmol) were dissolved in the mixture of 20 mL water, 8 mL ethanol and 20 mL toluene. After stirred in N₂ atmosphere for about 15 min, 47 mg (0.04 mmol) Tetrakis(triphenylphosphine)palladium(0) was added immediately. The mixture was refluxed in 70 °C for 18h. After extraction, the crude was dried by Na₂SO₄, condensed, and purified by chromatography using CH₂Cl₂: Petroleum ether (3/1; v/v) to obtain a yellow powder.

Compound 4a (DPNCANA): yield 69%, bright yellow powder, ¹H NMR (400 MHz, CDCl₃) δ 8.65 (dd, J = 15.2, 7.4 Hz, 4H), 8.52 – 8.39 (m, 4H), 8.35 (s, 2H), 7.83 (d, J = 7.7 Hz, 4H), 7.75 – 7.63 (m, 10H), 7.57 (dd, J = 12.7, 8.0 Hz, 8H), 4.33 – 4.15 (t, 4H), 1.89 – 1.67 (m, 4H), 1.43 – 1.26 (m, 20H), 0.87 (t, J = 7.1 Hz, 6H).

Compound 4b (DPCNCANA): yield 57%, orange yellow powder, ¹H NMR (400 MHz, CDCl₃) δ 8.66 (dd, J = 13.1, 7.4 Hz, 4H), 8.47 (s, 2H), 8.37 (d, J = 8.9 Hz, 4H), 8.00 (d, J = 8.4 Hz, 4H), 7.84 (dd, J = 17.9, 7.9 Hz, 8H), 7.72 – 7.58 (m, 8H), 4.24 – 4.18 (t, 4H), 1.77 (m, 4H), 1.44 (d, J = 14.6 Hz, 8H), 1.29 (m, 12H), 0.87 (t, J = 6.7 Hz, 6H).

Memory device fabrication

The indium-tin-oxide (ITO) glass was pre-cleaned with water, acetone, and alcohol in an ultrasonic bath for 30 min, respectively. The solution of 10 mg compounds in 1 mL *o*-dichlorobenzene was filtered through a microfilter equipped with a 0.22 μm sized pinhole. The solution was evaporated under high vacuum (10⁻³ Torr) and the film thickness was decided by the speed of the spin-coating machine. An aluminum layer was thermally evaporated and deposited onto the active film at about 10⁻⁷ Torr through a shadow mask to form the top electrode. The sandwich-structured memory device area of about 0.0314 mm² was obtained.



Scheme 1. Synthesis scheme and molecular structures of DPHCANA and DPCNCANA. Reagents and conditions: (a) FeCl₃, DCM, RT; (b) NBS, CHCl₃, ice water to RT; (c) NA, K₂CO₃, (PPh₃)₄Pd, H₂O, C₂H₅OH, toluene, 70 °C, under N₂ atmosphere.

Results and Discussion

Molecular structures and synthesis routes

Scheme 1 shows the molecular structures of DPHCANA and DPCNCANA, and the synthesis routes of both molecules. The detailed synthesis steps of the intermediates and the ^1H NMR spectra of DPHCANA and DPCNCANA are depicted in the *Supplementary Information* part.

Thermal properties

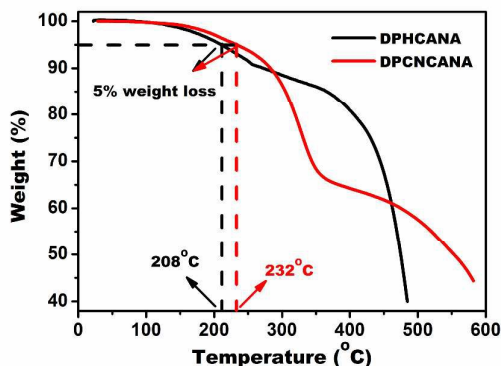


Fig. 1 TGA curves of the two small molecules under an air flow rate of 50 mL·min⁻¹.

Thermal properties were investigated by TGA, as shown in figure 1. The thermal decomposition temperatures with 5% weight loss were measured to be 208 °C and 232 °C for DPHCANA and DPCNCANA, respectively. The higher decomposition temperature of DPCNCANA maybe arises from the condensed molecular interactions in solid state.

Photophysical properties

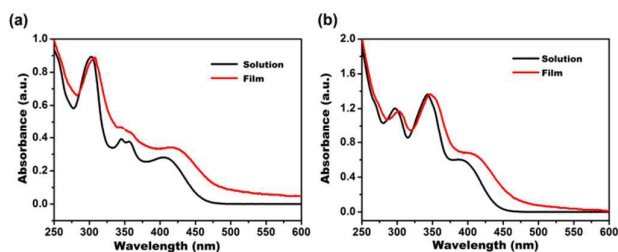


Fig. 2 UV-Vis absorption spectra of (a) DPHCANA and (b) DPCNCANA in tetrahydrofuran solution and film states.

The UV-vis absorption spectra of both molecules in tetrahydrofuran (THF) solution and in film states are shown in figure 2. As shown in Fig. 2a, the absorption peak located at 304 nm was attributed to the carbazole segment while that observed at 405 nm was consistent with the intramolecular charge transfer (ICT) from electron-donors to the electron-acceptors. Meanwhile, the shoulder peak between 332-379

nm was originated from the $n-\pi^*$ transition of C=O bonds in naphthalimide chromophore.²³ For DPCNCANA in solution (Fig. 2b), the absorption peak located at 349 nm was the combination of the $n-\pi^*$ electronic transition of C=O bonds in naphthalimide chromophore and the $n-\pi^*$ electronic transition of C=N bonds, leading to the largely increased absorption intensity. Additionally, the ICT peak located at 390 nm was blue-shifted when compared with that of DPHCANA (405 nm), and this was mainly caused by the increased dihedral angle that decreased the coplanarity and was not beneficial for the ICT throughout the molecular backbone. In comparison with their UV-vis spectra in solution, the absorption bands of DPCNCANA and DPHCANA in film were red-shifted 18 nm and 13 nm, respectively, and thus showing a strong intermolecular interaction in the DPCNCANA film state,²⁴ which maybe also arise from the more ordered intermolecular stacking than that of DPHCANA.

Electrochemical properties

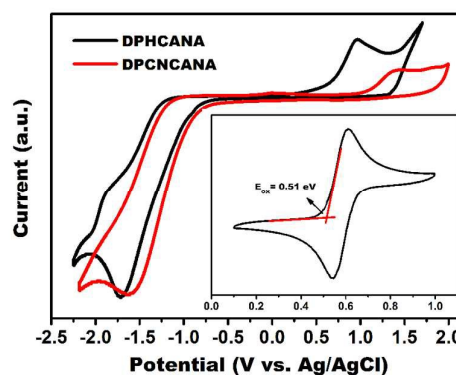


Fig. 3 Cyclic voltammogram of DPHCANA and DPCNCANA on ITO substrates in acetonitrile solution with 0.1M tetrabutylammonium perchlorate as electrolyte and ITO glass as the working electrode.

Cyclic voltammetry (CV) measurements were carried out to understand the electronic properties of the films spin-coated on ITO glasses in anhydrous acetonitrile solution. As we can see in figure 3, the onset oxidations (E_{onset}) of DPHCANA and DPCNCANA films are 0.73 eV and 1.12 eV, respectively. The highest occupied molecular orbital (HOMO) level and the lowest unoccupied molecular orbital (LUMO) level can be calculated by the equations: $\text{HOMO} = - [E_{\text{onset}} + 4.8 - E_{\text{Ferrocene}}]$, $\text{LUMO} = \text{HOMO} + E_g$. Where $E_{\text{Ferrocene}}$ is the ferrocene/ferrocenium redox standard potential which can be deduced from the inset of figure 3 and E_g is the optical bandgap which can be estimated from the onset of UV-Vis absorption spectra. The detailed CV data are summarized in Table 1.

The results are almost in accordance with the previous assumption; as the cyano group was introduced into the molecular backbone, the HOMO level decreased from -5.02 eV for DPHCANA to -5.41 eV for DPCNCANA, however, the energy gaps for both molecules are very close and only 0.07 eV different. As shown in Table 1, the energy barrier between

work function of ITO and HOMO energy levels for DPHCANA and DPCNCANA is 0.22 eV and 0.61 eV, respectively, both are much smaller than that between work function of Al and LUMO energy level being 1.84 eV and 1.52 eV, indicating that it is more convenient for hole injection from ITO into the HOMO levels of both molecules. Therefore, both molecules are dominated by hole-transporting and the hole injection barrier

for DPCNCANA is much higher than that of DPHCANA. According to this situation, the threshold voltage based on DPHCANA would be much smaller than that based on DPCNCANA. The LUMO of DPCNCANA is -2.76 eV which is much smaller than that of DPHCANA around at -2.46 eV, suggesting the DPCNCANA molecule has a better stability in the air ambient circumstance.

Table 1 Optical and electrochemical properties of the films fabricated with DPHCANA and DPCNCANA

Molecule	λ_{onset} (nm)	E_{g} (eV) ^a	E_{onset} (eV) ^b	HOMO (eV) ^c	LUMO (eV) ^d	$\Phi_{\text{Al-HOMO}}$ (eV)	LUMO- Φ_{Al} (eV)
DPHCANA	485	2.56	0.73	-5.02	-2.46	0.22	1.84
DPCNCANA	471	2.63	1.12	-5.41	-2.78	0.61	1.52

^a Estimated from the onset of absorption: bandgap = $1240/\lambda_{\text{onset}}$. ^b Potential vs. Ag/AgCl in a 0.1 M anhydrous acetonitrile solution of tetrabutylammonium perchlorate (TBAP). ^c The HOMO energy levels were calculated from cyclic voltammetry with reference to ferrocene (0.51 eV): HOMO = - [$E_{\text{onset}} + 4.8 - E_{\text{ferrocene}}$]. ^d LUMO = HOMO + E_{g} .

Current–voltage (*I*–*V*) characteristics of the memory devices

In order to verify the analysis of the CV measurements above, we measured the current-voltage (*I*-*V*) characteristics of memory devices fabricated with DPHCANA and DPCNCANA respectively. Figure S3a is the scheme of the sandwich-structured memory devices, which consists of an indium-tin oxide (ITO) bottom electrode, a spin-coated organic active-layer and an Al top electrode. The thickness of the spin-coated active layer is about 90 nm while that of Al electrode is estimated to be 150 nm according to the SEM image of the devices (Fig. S3b). The current-voltage (*I*-*V*) characteristics of ITO/DPHCANA/Al device were measured under an external electric field, as shown in Fig. 4a. The current was initially in low-conductivity (OFF) state, when a voltage from 0 to -5 V was applied on one cell of the device, a sharp increase in current was observed at switching threshold of -2.11 V, indicating the transition from low-conductivity (OFF) state to high-conductivity (ON) state (sweep 1). This electrical transition can serve as the “writing” process for ITO/DPHCANA/Al device. Upon reaching the high-conductivity state, the current still remained in the ON state in the subsequent voltage sweep (sweep 2). In the reverse voltage sweep from 0 to 5 V (sweep 3), an abrupt decrease in current was observed at a threshold voltage of about 2.74 V, which indicates that the memory device undergoes a transition from ON state to the original OFF state. This electrical transition serves as the “erase” process for data-storage devices. Therefore, the memory device fabricated with DPHCANA is a binary Flash data-storage device.

The current-voltage characteristics of the sandwich structured memory device fabricated with DPCNCANA were measured in the same condition (Fig. 4b). In the first voltage

sweep from 0 to -5.0 V, an abrupt current increase was observed at a threshold voltage of -2.23 V, indicating that this memory device undergoes a transition from low-conductivity state (OFF state) to intermediate-conductivity state (ON1 state). And the current could further increase to the high-conductivity state (ON2 state) with the voltage increasing to -2.86 V. The cell remained in this high-conductivity state during the subsequent scan from 0 to -5.0 V (sweep 2). The three current states can be corresponding to 0, 1 and 2 ternary data storage utilities. Sweep 3 was operated on another cell of the device over a voltage ranging from 0 to -2.7 V, and a sharp increase in current was showed at a threshold voltage of -2.28 V. The intermediate-conductivity stage was maintained during the subsequent scan from 0 to -2.7 V (sweep 4). Sweep 5 was carried out in the same cell of the device over a voltage from 0 to -5 V, an abrupt increase in current occurred from 10^{-4} A to 10^{-2} A at a switching threshold voltage of about -2.84 V. As long as the devices reaching the ON state, neither the subsequent voltage sweep (sweep 6) nor the reverse voltage sweep (sweep 7) would return the memory device to the original OFF state. Therefore, due to the introducing of CN group into the molecular backbone, we successfully fabricated a memory device with typical ternary WORM (write once read many times) memory behaviour. Additionally, no obvious degradation in current was observed for about 4 h under a constant stress of -1 V for both memory devices, as shown in Figure 5. Unexpectedly, the threshold voltage of DPCNCANA device is nearly the same as that of DPHCANA, which is not consistent with the analysis of the CV measurements above. To understand this phenomenon, measurements regarding the microstructures and the crystalline ordering of the two films were carried out.

Journal Name

ARTICLE

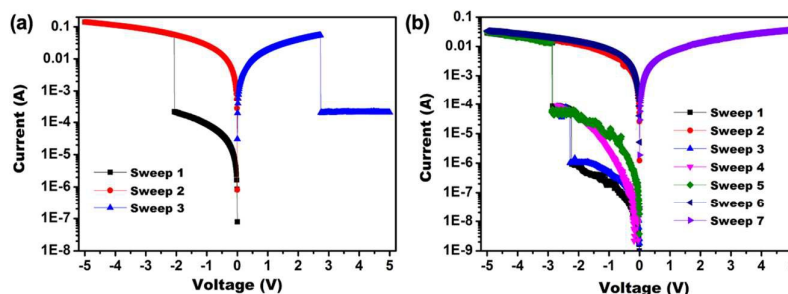


Fig. 4 The current-voltage (I-V) characteristics of the memory devices fabricated with (a) DPHCANA and (b) DPCNCANA.

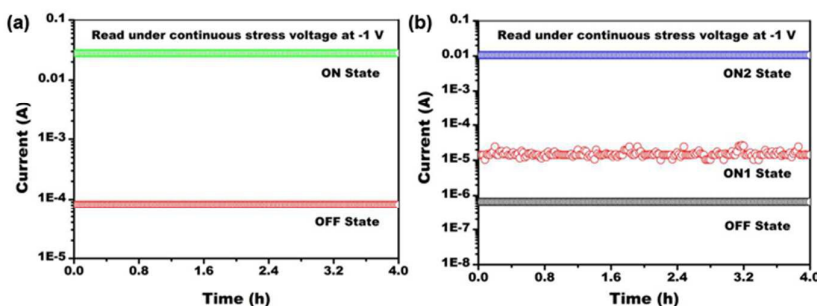


Fig. 5 Stability test of the memory devices in all states under stimulus by read pulses at -1 V; (a) DPHCANA and (b) DPCNCANA.

Morphology of the thin films

To characterize the microstructure of the spin-coated thin films of DPHCANA and DPCNCANA, atomic force microscopy (AFM) measurements were carried out. As shown in Fig. 6a, the surface morphology of DPHCANA film shows no distinct structure, indicating poor stacking in solid state. In contrast, figure 6b shows that DPCNCANA formed a well-organized grain-like structure, which is deduced to be resulted from the progressively ordered stacking by CN \cdots CN and CN \cdots H interactions. Thus, DPCNCANA formed a crystalline structure in the film state and the introducing of cyano groups into the molecular backbone resulted in the total different film surface morphology of DPCNCANA. In addition, the surface root-mean-square (RMS) roughness of DPCNCANA is estimated to be 1.69 nm. The ordered stacking and small RMS of DPCNCANA are beneficial to improve charge transport mobility through the organic active layers and decrease the energy barriers between the active layers and the electrodes. Thus, less power was needed to overcome the energy barrier and the threshold voltage of DPCNCANA based memory device was not much larger than that of DPHCANA.²⁵

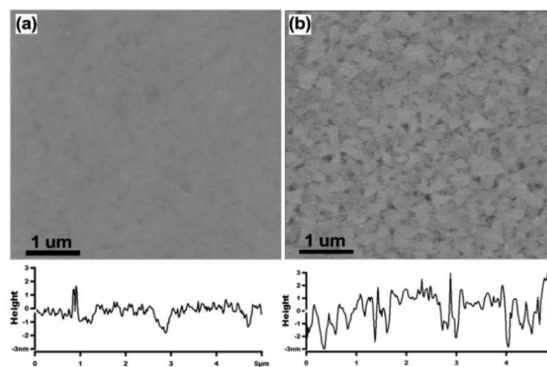


Fig. 6 The tapping-mode AFM height images of (a) DPHCANA and (b) DPCNCANA films spin-coated onto ITO glass.

IR spectra of the thin films

To demonstrate the intermolecular H-bond (H \cdots N-C) that was generated between the neighbouring molecules, we measured the IR absorbance spectra of molecule DPHCANA and

DPCNCANA in both solution and film states. Firstly, as shown in Figure S4, the IR absorbance spectrum of molecule DPHCANA in solution state was almost the same to that of the IR absorbance spectrum in film state. However, Figure S5 showed a little difference between the IR absorbance spectra of molecule DPCNCANA in film and solution states. Compared with the absorbance spectrum in solution state, the peak located at 2232 cm^{-1} arising from the CN group blue-shifted for about 6 cm^{-1} , as shown in Figure 7a. Additionally, the peak located between 2800 cm^{-1} and 3000 cm^{-1} that corresponds to the frequencies of C-H stretching mode also had a blue shift for about 6 cm^{-1} . These results demonstrate that intermolecular H-bond was generated in the films due to the introducing of CN groups in the molecular backbones.²⁶

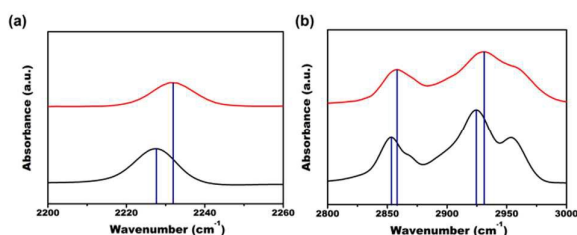


Fig. 7 IR absorbance spectra of DPCNCANA in solution and in film state. The red line represented the IR spectra in film state and the black line represented the IR in solution state. (a). CN-group. (b). C-H stretching mode.

Molecular stacking in the thin films

X-ray diffraction (XRD) measurements of the two molecules spin-coated on ITO substrates were performed to further understand the effects of CN groups in the molecular backbone (Figure 8). The diffraction peak observed at $2\theta = 18.96^\circ$ for molecule DPHCANA corresponded to a d -spacing of 4.67 \AA which indicated a relative ordered arrangement in the films. This result was mainly due to the large conjugated planarity of carbazole moieties. In addition, the diffraction peaks at $2\theta = 6.58^\circ$ (13.42 \AA), 9.89° (8.93 \AA), 13.19° (6.72 \AA) and 16.45° (5.38 \AA) are also observed for molecule DPCNCANA. The d -spacing of 5.38 \AA belongs to the microstructure ordering distance while the diffraction peak at $2\theta = 6.58^\circ$ (13.42 \AA) means a long-range order, which indicates that the ordered stacking is formed in solid state. Moreover, the $2\theta = 13.19^\circ$ is almost twice of $2\theta = 6.58^\circ$, indicating that DPCNCANA formed a well-organized layer by layer stacking in the film. This result may be caused by three reasons: (1) The large conjugated plane of carbazole moieties; (2) The alkyl chains serving as the spacer to control the distance of the conjugated backbones; (3) the strong π -stacking of molecules by $\text{CN}\cdots\text{CN}$ and $\text{CN}\cdots\text{H}$ interactions. Therefore, DPCNCANA self-assembled into ordered crystalline and formed close layer by layer stacking in the thin film state which is consistent with the UV analysis and the AFM image. The stacking of DPCNCANA in film state is beneficial for promoting the mobility of charge carriers, which also attributes to decrease the threshold voltage.

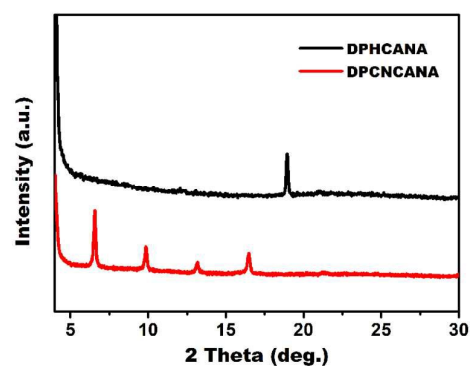


Fig. 8 The XRD patterns of DPHCANA and DPCNCANA films spin-coated onto ITO glass substrates.

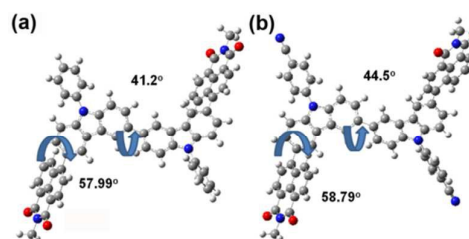


Fig. 9 The dihedral angles of DFT-optimized geometries of DPHCANA and DPCNCANA.

Density functional theory (DFT) method has been used in the theoretical calculations of B3LYP, with the 3-21G basis set to calculate the structural optimizations of these two molecules, as shown in figure 9. The dihedral angle between the carbazole core and the end-capping moiety naphthalimide group was nearly the same. At the meantime, the 9-phenylcarbazole derivative core of both DPHCANA and DPCNCANA possesses the nonplanar structure at ground state. The dihedral angle of DPCNCANA core is calculated to be 44.5° while that of DPHCANA core is estimated to be 41.2° . The larger dihedral angle means the larger twist of the molecular backbones and is not beneficial for decreasing the distance between the neighbouring molecules in film state, which may commendably explain the larger microstructure ordering distance for molecule DPCNCANA in the XRD measurements. Although the microstructure ordering distance of molecule DPHCANA is a little smaller than that of DPCNCANA, the stacking of molecule DPHCANA in film state is not as better as that of DPCNCANA. The stacking of the molecules in solid states is an extreme important element in the properties of the semi-conductive layers. Thus, due to the ordered crystalline stacking in the film state, the energy barriers that the charges should overcome through the films of DPCNCANA is smaller than that of DPHCANA, leading to the decreasing of the threshold voltage of the memory device. Thus, the threshold voltage of DPCNCANA is nearly the same as that of DPHCANA.

Proposed memory mechanisms

Finally, in order to better understand the electrical switching mechanism of the memory devices, electrostatic potential (ESP) surfaces and the HOMO and LUMO orbital surfaces of

DPHCANA and DPCNCANA were calculated through density functional theory with the B3LYP/3-21G basis set, as shown in Fig. 10. DFT molecular simulation results showed an open channel with continuous positive molecular electrostatic potential (in red) which is formed from the molecular surface throughout the conjugated backbone, indicating that the charge carriers can migrate through this open channel. Meantime, the negative molecular ESP regions (in blue) were attributed to the naphthalimide chromophores for molecule DPHCANA and to the naphthalimide chromophores and cyano groups for DPCNCANA. These negative regions can serve as the "traps" to block the mobility of the charge carriers, and the depth of these "traps" is in consistent with the electron-withdrawing ability of the electron-deficient groups.²⁷ For DPHCANA, the electron is initially located on the electron-donor carbazole moieties, and the "charge trap" arising from naphthalimide will be filled with electron quickly when an external voltage was applied on the cell of the device, which indicates that the current transits from OFF to ON state. The high conductivity state (ON state) is very stable, which exhibits

nonvolatile memory behaviour. Meantime, the current can be transitioned from the ON state back to the OFF state under the forward voltage, which indicates that the electron-withdrawing ability of naphthalimide group is weak and the trapped electron can be de-trapped in the reverse voltage. Therefore the device we fabricated with DPHCANA exhibits typical nonvolatile binary FLASH memory behaviour. For DPCNCANA, the transition from OFF state to ON1 state is the same to that of DPHCANA. Then the deep trap arising from cyano group will be filled with electron to full gradually with the increase of the voltage, leading to the transition from ON1 to ON2 state. Upon finishing the HOMO to LUMO+1 transition, the electron density distribution is mainly located on the cyano group and becomes more stable than initial state. Due to the strong electron-withdrawing ability of cyano group, the trapped electron is not easy to be de-trapped even the power is shut down or reversed, leading to a high conductivity state that can be maintained in a long time. Therefore the device we fabricated with DPCNCANA exhibits typical nonvolatile ternary WORM memory characteristics.

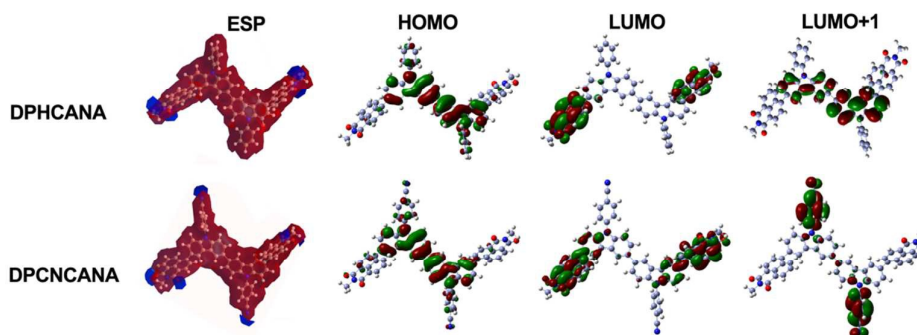


Fig. 10 Molecular electrostatic potential (ESP) surfaces and molecular orbital energy levels of DPHCANA and DPCNCANA.

Conclusions

In summary, we successfully synthesized two small molecules DPHCANA and DPCNCANA, the device based on cyano contained molecule DPCNCANA has a much lower HOMO value, however, happened intermolecular H-bond connection and led to molecular stacking and crystalline ordering in film state, which counteracted the negative effects of the higher hole transport barrier lying between the film HOMO level and the bottom electrode, achieved almost the same switch voltage with the counterpart molecule DPHCANA without cyano group. This result may provide a new strategy to synthesize conjugated molecules with novel structures and has the potential to play a vital role development of memory devices in the future.

Acknowledgements

This work was financially supported by the NSF of China (21176164, 21206102, 21336005 and 21476152), the NSF of Jiangsu Province (BE2013052), a project supported by the

Specialized Research Fund for the Doctoral Program of Higher Education of China (Grant No. 20123201120005), Chinese-Singapore Joint Project (2012DFG41900) and National Excellent Doctoral Dissertation funds (201455).

Notes and references

- 1 T. Osaka, M. Takai, K. Hayashi, K. Ohashi, M. Saito and K. Yamada, *Nature*, 1998, **392**, 796-798.
- 2 M. Emmelius, G. Pawlowski and H. W. Vollmann, *Angew. Chem. Int. Edit.*, 1989, **28**, 1445-1471.
- 3 G. Wang, S. F. Miao, Q. J. Zhang, H. F. Liu, H. Li, N. J. Li, Q. F. Xu, J. M. Lu and L. H. Wang, *Chem. Commun.*, 2013, **49**, 9470-9472.
- 4 Q. D. Ling, D. J. Liaw, C. X. Zhu, D. S. H. Chan, E. T. Kang and K. G. Neoh, *Prog. Polym. Sci.*, 2008, **33**, 917-978.
- 5 J. Q. Liu, Z. Y. Yin, X. H. Cao, F. Zhao, L. H. Wang, W. Huang and H. Zhang, *Adv. Mater.*, 2013, **25**, 233-238.
- 6 S. G. Hahm, S. Choi, S. H. Hong, T. J. Lee, S. Park, D. M. Kim, W. S. Kwon, K. Kim, O. Kim and M. Ree, *Adv. Funct. Mater.*, 2008, **18**, 3276-3282.

COMMUNICATION

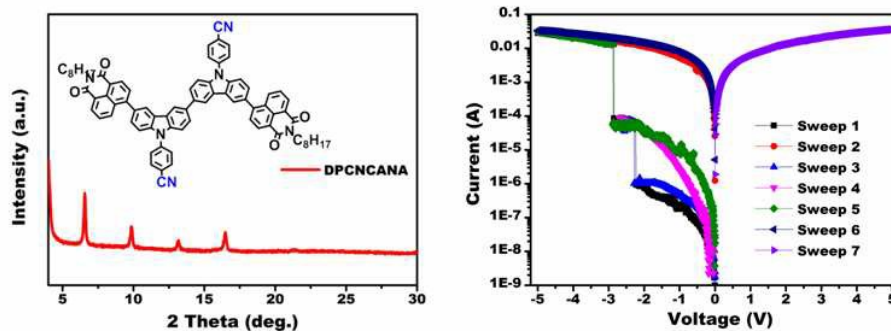
Journal Name

- 7 H. Li, Q. F. Xu, N. J. Li, R. Sun, J. F. Ge, J. M. Lu, H. W. Gu and F. Yan, *J. Am. Chem. Soc.*, 2010, **132**, 5542-5543.
- 8 S. F. Miao, H. Li, Q. F. Xu, Y. Y. Li, S. J. Ji, N. J. Li, L. H. Wang, J. W. Zheng and J. M. Lu, *Adv. Mater.*, 2012, **24**, 6210-6215.
- 9 P. Y. Gu, F. Zhou, J. K. Gao, G. Li, C. Y. Wang, Q. F. Xu, Q. C. Zhang and J. M. Lu, *J. Am. Chem. Soc.*, 2013, **135**, 14086-14089.
- 10 S. F. Miao, H. Li, Q. F. Xu, N. J. Li, J. W. Zheng, R. Sun, J. M. Lu and C. M. Li, *J. Mater. Chem.*, 2012, **22**, 16582-16589.
- 11 S. F. Miao, H. Li, Q. F. Xu, Y. Y. Li, S. J. Ji, N. J. Li, L. H. Wang, J. W. Zheng and J. M. Lu, *Adv. Mater.*, 2012, **24**, 6210-6215.
- 12 Y. H. Zhang, H. Zhuang, Y. Yang, X. F. Xu, Q. Bao, N. J. Li, H. Li, Q. F. Xu, J. M. Lu and L. H. Wang, *J Phys Chem C*, 2012, **116**, 22832-22839.
- 13 H. F. Liu, H. Zhuang, H. Li, J. M. Lu and L. H. Wang, *Phys Chem Chem Phys*, 2014, **16**, 17125-17132.
- 14 T. Lei, J. Y. Wang and J. Pei, *Accounts Chem Res*, 2014, **47**, 1117-1126.
- 15 (a) C. R. Newman, C. D. Frisbie, D. A. da Silva, J. L. Bredas, P. C. Ewbank and K. R. Mann, *Chem. Mater.*, 2004, **16**, 4436-4451. (b) Y. Yamashita, *Sci Technol Adv Mat*, 2009, **10**. (c) M. Y. Kuo, H. Y. Chen and I. Chao, *Chem-Eur. J.*, 2007, **13**, 4750-4758.
- 16 (a) G. R. Hutchison, M. A. Ratner and T. J. Marks, *J. Am. Chem. Soc.*, 2005, **127**, 2339-2350. (b) X. H. Zhang, Q. S. Li, J. B. Ingels, A. C. Simmonett, S. E. Wheeler, Y. M. Xie, R. B. King, H. F. Schaefer and F. A. Cotton, *Chem. Commun.*, 2006, DOI: Doi 10.1039/B515843e, 758-760.
- 17 T. M. Barclay, A. W. Cordes, C. D. MacKinnon, R. T. Oakley and R. W. Reed, *Chem. Mater.*, 1997, **9**, 981-990.
- 18 J. Q. Ding, B. H. Zhang, J. H. Lu, Z. Y. Xie, L. X. Wang, X. B. Jing and F. S. Wang, *Adv. Mater.*, 2009, **21**, 4983-4986.
- 19 B. J. Song, H. M. Song, I. T. Choi, S. K. Kim, K. D. Seo, M. S. Kang, M. J. Lee, D. W. Cho, M. J. Ju and H. K. Kim, *Chem-Eur. J.*, 2011, **17**, 11115-11121.
- 20 (a) G. Wang, S. F. Miao, Q. J. Zhang, H. F. Liu, H. Li, N. J. Li, Q. F. Xu, J. M. Lu and L. H. Wang, *Chem. Commun.*, 2013, **49**, 9470-9472. (b) M. Xu, J. M. Han, Y. Q. Zhang, X. M. Yang and L. Zang, *Chem. Commun.*, 2013, **49**, 11779-11781.
- 21 M. J. Frisch, G. W. Trucks, H. B. Schlegel, G. E. Scuseria, M. A. Robb, J. R. Cheeseman, J. A. Montgomery, Jr., T. Vreven, K. N. Kudin, J. C. Burant, J. M. Millam, S. S. Iyengar, J. Tomasi, V. Barone, B. Mennucci, M. Cossi, G. Scalmani, N. Rega, G. A. Petersson, H. Nakatsuji, M. Hada, M. Ehara, K. Toyota, R. Fukuda, J. Hasegawa, M. Ishida, T. Nakajima, Y. Honda, O. Kitao, H. Nakai, M. Klene, X. Li, J. E. Knox, H. P. Hratchian, J. B. Cross, V. Bakken, C. Adamo, J. Jaramillo, R. Gomperts, R. E. Stratmann, O. Yazyev, A. J. Austin, R. Cammi, C. Pomelli, J. W. Ochterski, P. Y. Ayala, K. Morokuma, G. A. Voth, P. Salvador, J. J. Dannenberg, V. G. Zakrzewski, S. Dapprich, A. D. Daniels, M. C. Strain, O. Farkas, D. K. Malick, A. D. Rabuck, K. Raghavachari, J. B. Foresman, J. V. Ortiz, Q. Cui, A. G. Baboul, S. Clifford, J. Cioslowski, B. B. Stefanov, G. Liu, A. Liashenko, P. Piskorz, I. Komaromi, R. L. Martin, D. J. Fox, T. Keith, M. A. Al-Laham, C. Y. Peng, A. Nanayakkara, M. Challacombe, P. M. W. Gill, B. Johnson, W. Chen, M. W. Wong, C. Gonzalez, and J. A. Pople, Gaussian 03, revision B.04, Gaussian, Inc., Wallingford CT, 2004.
- 22 B. Miehlich, A. Savin, H. Stoll and H. Preuss, *Chem. Phys. Lett.*, 1989, **157**, 200-206.
- 23 (a) M. S. Alexiou, V. Tychopoulos, S. Ghorbanian, J. H. P. Tyman, R. G. Brown and P. I. Brittain, *J. Chem. Soc. Perk. T. 2*, 1990, DOI: Doi 10.1039/P29900000837, 837-842. (b) B. Ramachandram, G. Saroja, N. B. Sankaran and A. Samanta, *J Phys Chem B*, 2000, **104**, 11824-11832.
- 24 (a) M. Surin, P. Sonar, A. C. Grimsdale, K. Mullen, S. De Feyter, S. Habuchi, S. Sarzi, E. Braeken, A. V. Heyen, M. Van der Auweraer, F. C. De Schryver, M. Cavallini, J. F. Moulin, F. Biscarini, C. Femoni, L. Roberto and P. Leclere, *J. Mater. Chem.*, 2007, **17**, 728-735. (b) R. Schmidt, J. H. Oh, Y. S. Sun, M. Deppisch, A. M. Krause, K. Radacki, H. Braunschweig, M. Konemann, P. Erk, Z. A. Bao and F. Wurthner, *J. Am. Chem. Soc.*, 2009, **131**, 6215-6228.
- 25 W. B. Zhang, C. Wang, G. Liu, X. J. Zhu, X. X. Chen, L. Pan, H. W. Tan, W. H. Xue, Z. H. Ji, J. Wang, Y. Chen and R. W. Li, *Chem. Commun.*, 2014, **50**, 11856-11858.
- 26 (a) D. Yokoyama, H. Sasabe, Y. Furukawa, C. Adachi, J. Kido, *Adv. Funct. Mater.*, 2011, **21**, 1375. (b) P. Hobza, Z. Havlas, *Chem. Rev.*, 2000, **100**, 4253. (c) X. S. Li, L. Liu, H. B. Schlegel, *J. Am. Chem. Soc.*, 2002, **124**, 9639.
- 27 X. D. Zhuang, Y. Chen, G. Liu, B. Zhang, K. G. Neoh, E. T. Kang, C. X. Zhu, Y. X. Li and L. J. Niu, *Adv. Funct. Mater.*, 2010, **20**, 2916-2922.

Dramatic achievement of stable ternary data storage material mediated by simply cyano group substitution

Qijian Zhang, Hao Zhuang, Jinghui He, Shugang Xia, Hua Li,* Najun Li, Qingfeng Xu and Jianmei Lu*

Table of Contents



Novelty: the forming of layer by layer stacking and the realization of excellent ternary memory device through introducing CN group in the molecular backbone.